Measurement of the Lower Hybrid Wave Using RF Magnetic Probes on the TST-2 Spherical Tokamak*)

Yongtae KO, Naoto TSUJII, Satoru YAJIMA, Yuichi TAKASE, Akira EJIRI, Osamu WATANABE, Hibiki YAMAZAKI, Charles P. MOELLER[1)], Yasuo YOSHIMURA[2)], Yusuke YOSHIDA, Yusuke IIDA, Kotaro IWASAKI, Yuya KAWAMATA, Sho SAKAMOTO, Yuki AOI, Teruki OISHI, Kyohei MATSUZAKI and James RICE

The University of Tokyo, Kashiwa 277-8561, Japan
[1)]*General Atomics, San Diego, CA 92186, USA*
[2)]*National Institute for Fusion Science, Toki 509-5292, Japan*

(Received 10 January 2019 / Accepted 8 May 2019)

Polarization-resolved spatial distribution of waves in the lower hybrid frequency range was measured using radio frequency magnetic probes (RFMPs) in the TST-2 spherical tokamak. Thirteen RFMPs were installed inside of the vacuum vessel, eight on the inboard-side, three on the outboard-side and two on the bottom-side. In TST-2, the lower hybrid wave (LHW) is excited by the outboard-launch antenna and the top-launch antenna. Higher plasma currents can be achieved using the top-launch antenna. Bottom-launch can be simulated by reversing the direction of the toroidal magnetic field. Propagation and absorption of the LHW were investigated numerically for outboard-, top-, and simulated bottom-launch at low and high plasma currents. Results of the wave measurement revealed different propagation characteristics for different launching, which agree partially with the results of numerical calculation.

Keywords: spherical tokamak, lower hybrid wave, magnetic probe

DOI: 10.1585/pfr.14.3402107

1. Introduction

Fully non-inductive plasma start-up and current drive is a major issue for the spherical tokamak (ST) since the elimination of the central solenoid (CS) for inductive current drive is considered necessary for the ST-based fusion reactor. On the TST-2 spherical tokamak, non-inductive plasma current (I_p) ramp-up using the lower hybrid wave (LHW (200 MHz)) is being studied [1]. Two capacitively-coupled combline (CCC) antennas, located on the outboard side (outboard-launch) and on the top side (top-launch), are used to excite the LHW. Furthermore, bottom launch can be simulated using the top-launch antenna by reversing the direction of the toroidal magnetic field B_t. According to ray-tracing calculation using GENRAY [2], wave propagation and current drive characteristics are clearly different among outboard launch, top launch and simulated bottom launch [3]. In order to identify the optimum scenario for I_p ramp-up, the LHW and the fast wave (FW) were measured by RF magnetic probes (RFMPs). In addition to wave power, phase, and frequency spectrum, wave polarization can be measured by RFMPs [4]. In this study, the global distributions of the LHW and the FW are measured using thirteen RFMPs installed inside the vacuum vessel and compared with predictions of numerical calculation. Experimental data were generally consistent with numerical calculation results of wave propagation and polarization.

2. Experimental Setup

Thirteen RFMPs were used in this experiment. Each RFMP consists of a single-turn coil formed by connecting the inner conductor to the outer conductor of a semi-rigid coaxial cable, metal enclosure for shielding, and a slit oriented in either toroidal or poloidal direction to select the RF magnetic field with particular polarization.

On the inboard side, eight RFMPs (10 mm × 15 mm rectangular loop) are arranged symmetrically about the mid-plane $z = 0$, as shown in Fig. 1. The (R, z) coordinates of RFMPs are $\mathrm{MP_{upper}}$: (+575, +100), $\mathrm{MP_{middle}}$: (+585, 0), $\mathrm{MP_{lower}}$: (+575, −100) on the outboard side, $\mathrm{MP_{in}}$: (+329, −450), $\mathrm{MP_{out}}$: (+535, −450) on the bottom side, and $\mathrm{A_{pol}}$: (+113, +327), $\mathrm{B_{\phi}}$: (+113, +177), $\mathrm{C_{pol}}$: (+113, +177), D: (+113, +27), $\mathrm{E_{\phi}}$: (+113, −27), $\mathrm{F_{\phi}}$: (+113, −177), $\mathrm{G_{pol}}$: (+113, −177), $\mathrm{H_{pol}}$: (+113, −327) on the inboard side. RFMPs on the outboard side and the bottom side consist of a single-turn coil wound around a teflon bobbin, and a metal enclosure with a slit in the poloidal direction. All RFMPs are located in the poloidal plane at a toroidal angle $\phi = -90°$ measured from the center of the outboard-launch

author's e-mail: ko@fusion.k.u-tokyo.ac.jp

*) This article is based on the presentation at the 27th International Toki Conference (ITC27) & the 13th Asia Pacific Plasma Theory Conference (APPTC2018).

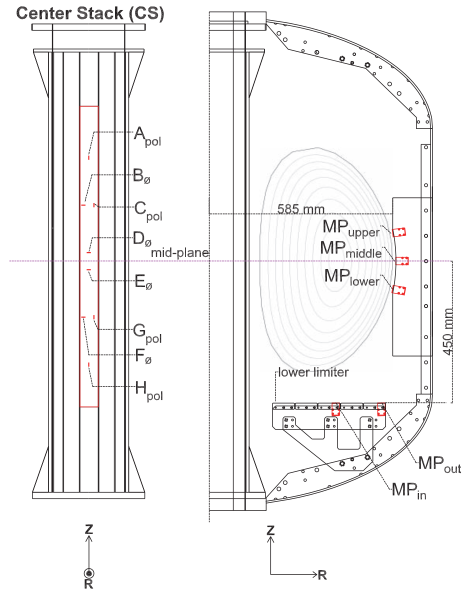

Fig. 1 Poloidal cross section of the vacuum vessel and a radial view of the inboard wall showing the locations of the limiters and RFMPs.

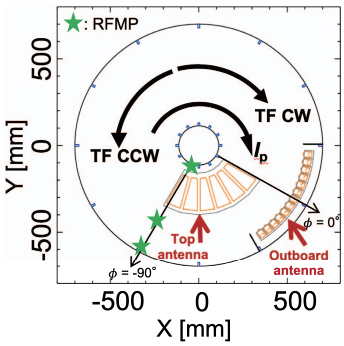

Fig. 2 RFMP and antenna locations viewed from the top.

antenna (Fig. 2).

The RF signals are measured by two oscilloscopes with bandwidths 500 MHz at 500 MSamples per second with 1 MWord memory (2 ms observation window) around t = 60 ms where I_p reaches the maximum value. The signal intensity is evaluated by integrating the frequency spectrum from 199 MHz to 201 MHz. To measure the signals obtained by all thirteen RFMPs, four reproducible shots are required due to the limited number of the oscilloscope channels.

3. Wave Measurement Results

The time evolution of the typical non-inductive I_p ramp-up discharge, comparing different cases of LHW launching, is shown in Fig. 3. In this series of experiment, low and high I_p case was investigated for each launching condition, though the I_p could not be controlled to be the same for each launching condition, with plasma currents of 5.5 kA to 11.7 kA for outboard launch (CW B_t), 6.3 kA to 19 kA for top launch (CW B_t), and 6.8 kA to 14 kA for simulated bottom launch (top launch with CCW B_t). The H_{pol} RFMP was out of order for the top-launch experiment with CW B_t.

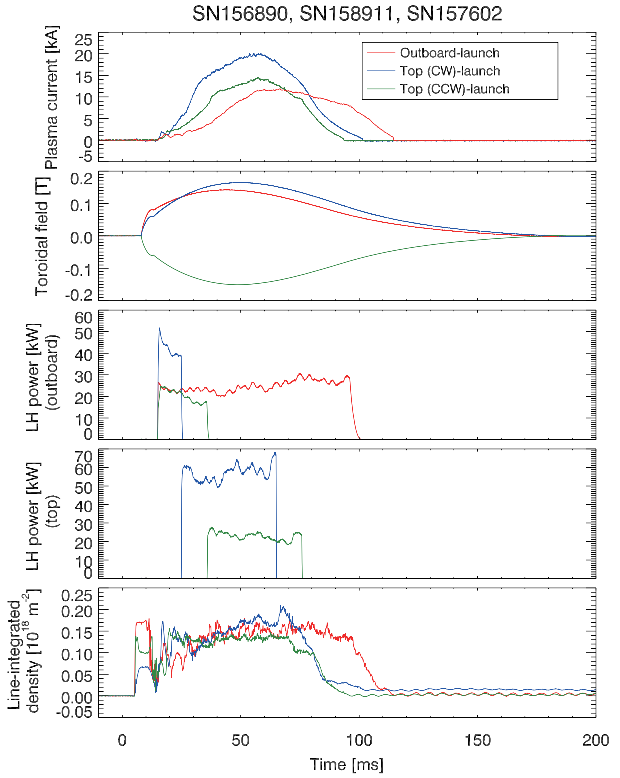

Fig. 3 Evolutions of typical non-inductive I_p ramp-up discharges. Red, blue and green lines indicate outboard-launch, top-launch (with CW B_t) and top-launch (with CCW B_t), respectively. The last case simulates bottom-launch.

Figure 4 summarizes the RF signal intensities measured by the thirteen RFMPs. As shown on the right figure, the horizontal axis on the left figure is the distances from the midplane on the inboard side defined as the origin, measuring downward, then radially outward through RFMPs MP_{in} and MP_{out}, and finally vertically upward to the topmost RFMP on the outboard side (MP_{upper}). The vertical axis on the left figure is the measured RF signal intensity normalized by the injected LHW power. The normalized RF signal intensities are plotted for low I_p and high I_p. The background noise level was measured in the absence of RF power injection. The signal level is at least two orders of magnitude greater than the noise level.

In the case of outboard-launch, the poloidal magnetic field component is largest at MP_{lower} and MP_{out}. This result suggests that the LHW injected from outboard side propagates downward. It has been observed previously that the RF magnetic field has a poloidal polarization around these locations as expected from LHW launch [4]. After passing through outboard and bottom regions of the plasma, the wave reaching the inboard side has a strong toroidal

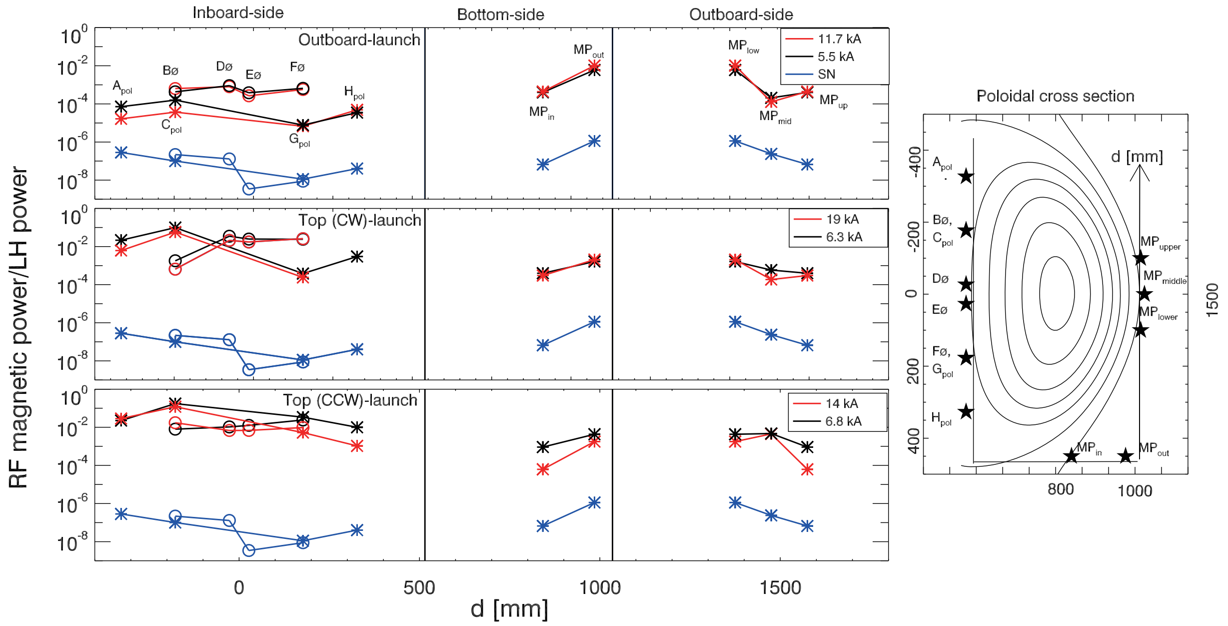

Fig. 4 I_p dependence of RF signal intensity for different wave launching modes. The horizontal axis in the left figure represents the distance from midplane downward, radially outward, then upward through RFMPs as shown on the right figure which also shows the locations of RFMPs on the poloidal cross section. Symbols of circle and asterisk indicate the slit along toroidal and poloidal direction, respectively. The vertical axis is the RF signal intensity normalized by the LHW injection power. The noise level measured without RF power injection is shown for each probe.

polarization which now appears to correspond to the FW polarization. The poloidally polarized component (corresponding to the LHW polarization) measured at the upper inboard-side by C_{pol} and A_{pol} becomes weaker at higher I_p. This may indicate stronger damping of the LHW at higher I_p predicted by the numerical analysis shown in the next section.

In the case of top launch, the RF power intensity measured by RFMPs in the upper half of the inboard side is over 100 times greater than in the case of outboard launch. The poloidal polarization is largest at C_{pol}. The RF power intensity is two orders of magnitude less at $B_ø$, compared to C_{pol} which is right next to $B_ø$. In the lower inboard region, toroidal polarization becomes larger. The measured overall signal intensity becomes weaker as the distance from the top-launch antenna increases as expected naturally from the damping of LHW. The signal decreases at higher I_p which is consistent with stronger absorption predicted theoretically. Significant differences could not be seen between outboard launch and top launch by RFMPs in the bottom and outboard regions.

Obvious differences can be seen for top launch when the direction of B_t is reversed from CW to CCW (CCW B_t corresponds to simulated bottom launch). For simulated bottom launch, the degree of polarization is weaker, and the RF signal intensity measured in the lower inboard region becomes larger than outboard launch and top launch. This indicates that the absorption is substantially weaker for CCW B_t compared to CW B_t. The RF signal intensity decreases at lower half of the plasma by an order of magnitude at higher I_p, which suggests that stronger absorption is recovered at higher I_p.

4. Comparison with Numerical Calculation

Results of ray-tracing calculation using GENRAY are shown in Fig. 5. Each experimental sections performed in Sec. 3 were simulated. The ray trajectories are projected on a poloidal cross section, and the rays with 70% of the maximum power are shown. Figures 5 (a) and 5 (b) show the outboard launch case with CW B_t with high I_p and low I_p. The top launch case with CW B_t with high I_p and low I_p and also CCW B_t with high I_p and low I_p are shown in Figs. 5 (c-f). The color bar indicates the degree of polarization towards B_z defined as

$$\theta_{pol} = \frac{180}{\pi} \mathrm{atan}\left(\frac{|B_z|}{|B_ø|}\right), \tag{1}$$

where B_z and $B_ø$ are calculated from the dispersion relation.

For outboard launch case, rays have $\theta_{pol} = 60°$ polarization initially and propagate toward lower half of the plasma regardless of the I_p. This agrees with the experimental data shown in Sec. 3. However, the poloidal polarization becomes dominant close to the inboard side, whereas in the experiment, toroidal polarization is dominant. This suggests that mode conversion of LHW to FW is not accounted for properly in the numerical model. Further measurement and modeling are required to clarify this point.

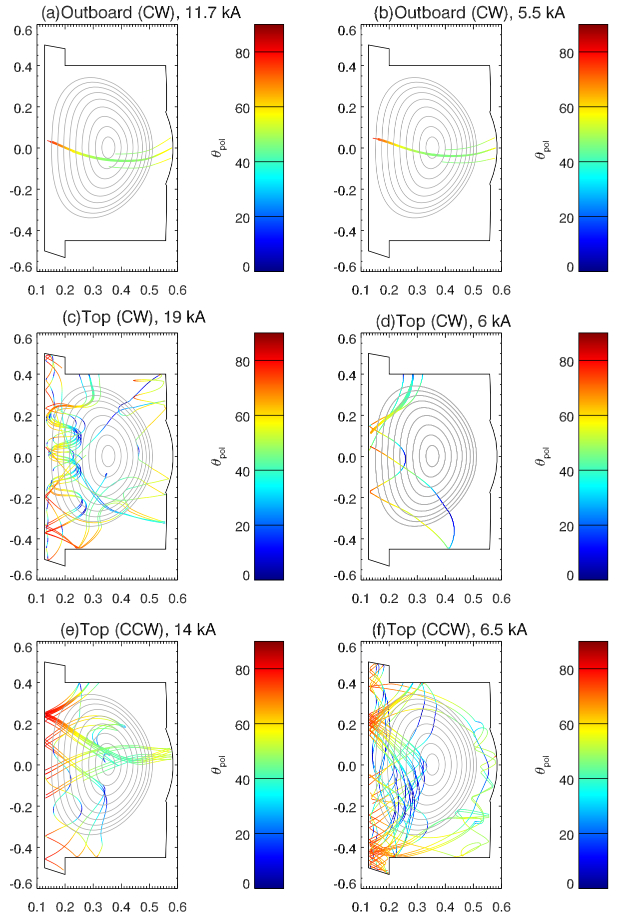

Fig. 5 Results of ray-tracing calculation using GENRAY for (a) outboard launch with CW B_t and high I_p, (b) with low I_p, (c) top launch with CW B_t and high I_p, (d) CW B_t and low I_p, (e) CCW B_t and high I_p, and (f) CCW B_t and low I_p. The color bar indicates the degree of polarization towards B_z (Eq. (1)).

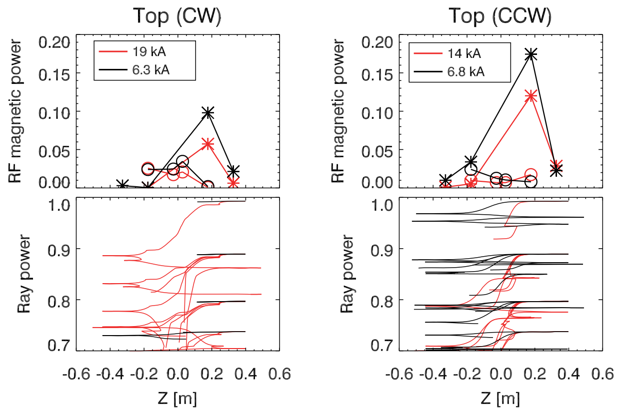

Fig. 6 Comparison of RF power which were measured experimentally and calculated numerically for top (CW) and top (CCW) cases. The RF power is plotted in linear scale and the ray power is normalized by the initial power.

For top launch with CW B_t, rays reach the upper inboard side around $z = +0.2$ m with dominantly poloidal RF magnetic field polarization. In the range between $z = +0.2$ m and $z = -0.2$ m polarization becomes dominantly toroidal in the core, the rays turn around radially, and polarization becomes more poloidal near the inboard wall. Toroidal, poloidal, and intermediate polarization exist in this region. This alternation of polarization direction can also be seen in Fig. 4 for the top (CW) case. At low I_p, up-shift of the parallel refractive index was weaker, resulting in weaker absorption. Therefore the RF signal intensity is expected to be larger than high I_p.

For top launch with CCW B_t, at high I_p, the RF magnetic field polarization is dominantly poloidal in the upper inboard region. The wave power decreases as the rays move downward. A comparison between the calculated ray powers and the measured RF powers are shown in Fig. 6 for top (CW) and top (CCW) cases. In this figure, the RF power is plotted in linear scale and the ray power is normalized by the initial power. Damping of the ray power can be seen as rays travel downward. At high I_p, rays which are reflected around $z = +0.2$ m propagate towards the plasma center and to the outboard region, and are reflected at the outboard edge again. At low I_p, rays which are reflected around $z = +0.2$ m propagate downward and fill the inboard bottom region more density compared to the high I_p case as shown in Figs. 5 (e) and (f). These results agree with the experimental observation that the RF signal intensity in the lower inboard region is an order of magnitude higher at low I_p than at high I_p.

5. Summary

Wave measurements were performed on TST-2 using RFMPs for three different modes of LHW excitation, outboard launch, top launch, and simulated bottom launch (top launch with reversed B_t). In particular, RFMPs on the inboard side could measure wave polarization. Experimentally, different characteristics were observed depending on LHW excitation mode and I_p. Measured powers on the outboard RFMPs and bottom RFMPs did not vary significantly among different LHW excitation modes. In contrast, RF power distribution measured by inboard RFMPs changed drastically for different excitation modes. RF signal intensities detected by inboard RFMPs were much stronger for top launch compared to outboard launch. RF signal intensity and polarization were compared with results of numerical calculation.

For outboard launch with CW B_t and high I_p, results of ray-tracing calculation are partially consistent to experimental results that wave propagate in the lower plasma region. On the other hand, the polarization of RF magnetic field on the inboard side did not agree with the ray-tracing calculation. Possibility of mode conversion to FW needs to be investigated further. For top launch with CW B_t and high I_p, results of ray-tracing calculation are consistent with experimental observation. RF magnetic field polarization on the inboard side is dominantly poloidal in the upper region, becomes more toroidal in the middle region near the midplane, and dominantly poloidal again in the lower region. For top launch with CCW B_t, results of ray-tracing were again consistent with experimental data. The wave power is strong in the upper inboard region. The comparison of ray powers shown in Fig. 6 implies that ramp up to higher current may be achieved for the top (CCW) case than either the outboard case and the top (CW) case since ray power damping is stronger. Rays with down-shifted parallel wavenumber fill a broad range of edge plasma on the inboard side at low I_p, and the RF signal intensity decreased as I_p increased. RF signal intensities detected by outboard and bottom RFMPs were similar for both top (CW) and top (CCW) cases.

In conclusion, spatial distributions of wave power, phase, frequency spectrum, and wave polarization were measured by thirteen RFMPs surrounding the plasma cross section. In particular, wave propagation changed drastically depending on I_p except for the outboard launch case, but experimentally, the dependency of RF power distribution on I_p could not be seen apart from reduction in amplitude. In order to resolve this discrepancy and to make a more quantitative comparison, expansion of the RFMP system for higher spatial and polarization coverage is necessary. This will contribute to identify optimum I_p ramp-up scenario.

Acknowledgement

This work is supported by Grant-in-Aid for Scientific Research (S) (21226021), by National Institute for Fusion Science Collaboration Research Programs NIFS14KOCR001, NIFS18KOAR022 and NIFS12KUTR078. This work is also supported in part by Japan/US Cooperation in Fusion Research and Development and US DoE Cooperative Agreement DE-FC02-04ER54698.

[1] Y. Takase *et al.*, Nucl. Fusion **53**, 063006 (2013).
[2] A.P. Smirnov *et al.*, 1994 GENRAY Code www.compxco.com/genray.html
[3] S. Yajima *et al.*, Plasma Fusion Res. **13**, 1202093 (2018).
[4] T. Shinya *et al.*, Plasma Fusion Res. **9**, 3402040 (2014).